

Radio Luminosity, Black Hole Mass and Eddington Ratio for Quasars from the Sloan Digital Sky Survey *

Wei-Hao Bian^{1,2}, Yan-Mei Chen², Chen Hu³, Kai Huang¹ and Yan Xu¹

¹ Department of Physics and Institute of Theoretical Physics, Nanjing Normal University, Nanjing 210097, China; bianwh@ihep.ac.cn

² Key Laboratory for Particle Astrophysics, Institute of High Energy Physics, Chinese Academy of Sciences, Beijing 100049, China

³ National Astronomical Observatories, Chinese Academy of Sciences, Beijing 100012, China

Received 2007 October 27; accepted 2008 March 19

Abstract We investigate the $M_{\text{BH}}-\sigma_*$ relation for radio-loud quasars with redshift $z < 0.83$ in Data Release 3 of the Sloan Digital Sky Survey (SDSS). The sample consists of 3772 quasars with better models of the $\text{H}\beta$ and $[\text{O III}]$ lines and available radio luminosity, including 306 radio-loud quasars, 3466 radio-quiet quasars with measured radio luminosity or upper-limit of radio luminosity (181 radio-quiet quasars with measured radio luminosity). The virial supermassive black hole mass (M_{BH}) is calculated from the broad $\text{H}\beta$ line, and the host stellar velocity dispersion (σ_*) is traced by the core $[\text{O III}]$ gaseous velocity dispersion. The radio luminosity and radio loudness are derived from the FIRST catalog. Our results are as follows: (1) For radio-quiet quasars, we confirm that there is no obvious deviation from the $M_{\text{BH}}-\sigma_*$ relation defined for inactive galaxies when the uncertainties in M_{BH} and the luminosity bias are concerned. (2) We find that the radio-loud quasars deviate more from the $M_{\text{BH}}-\sigma_*$ relation than do the radio-quiet quasars. This deviation is only partly due to a possible cosmological evolution of the $M_{\text{BH}}-\sigma_*$ relation and the luminosity bias. (3) The radio luminosity is proportional to $M_{\text{BH}}^{1.28^{+0.23}_{-0.16}} (L_{\text{Bol}}/L_{\text{Edd}})^{1.29^{+0.31}_{-0.24}}$ for radio-quiet quasars and to $M_{\text{BH}}^{3.10^{+0.60}_{-0.70}} (L_{\text{Bol}}/L_{\text{Edd}})^{4.18^{+1.40}_{-1.10}}$ for radio-loud quasars. The weaker dependence of the radio luminosity on the mass and the Eddington ratio for radio-loud quasars shows that other physical effects would account for their radio luminosities, such as the spin of the black hole.

Key words: quasars: emission lines — galaxies: nuclei — galaxies: bulges — black hole physics

1 INTRODUCTION

The relation between the mass of a supermassive black hole (SMBH) and the stellar velocity dispersion of its host (hereafter $M_{\text{BH}}-\sigma_*$ relation) is one of the most important results in the study of SMBHs in recent decades. It implies an intimate correlation between the SMBHs and their host galaxies (e.g. Gebhardt et al. 2000; Ferrarese & Merrit 2000; Tremaine et al. 2002; Lauer et al. 2007). This correlation would provide strong constraints on the evolution of active galactic nuclei (AGN). However, its reality is still under debate for different kinds of AGN, such as radio-loud AGNs, narrow-line Seyfert 1 galaxies, intermediate supermassive black hole, etc. (see e.g., Nelson 2001; Boroson 2003; Shield et al. 2003; Bian & Zhao 2004; Grupe & Mathur 2004; Bonning et al. 2005; Greene & Ho 2006; Woo et al. 2006; Zhou et al. 2006; Salviander et

* Supported by the National Natural Science Foundation of China.

al. 2007; Komossa & Xu 2007; Shen et al. 2008). In order to check this relation for the AGN, we should calculate M_{BH} and σ_* as accurately as possible.

The width of the broad emission lines (e.g., $\text{H}\beta$, $\text{H}\alpha$, Mg II , C IV) can be used to trace the virial velocity of the clouds in the broad line regions (BLRs) when the contribution from the narrow-line regions (NLRs) is reasonably removed, and the reverberation mapping method or the empirical luminosity-size relation can be used to calculate the BLRs size (e.g., Kaspi et al. 2000; McLure & Dunlop 2004; Bian & Zhao 2004; Peterson et al. 2004; Greene & Ho 2005b). The gas velocity dispersion of the narrow lines (e.g., $[\text{O III}]$, $[\text{O II}]$, $[\text{S II}]$) from the NLRs are usually used to trace the host stellar velocity dispersion (e.g., Nelson & Whittle 1996; Greene & Ho 2005a). We also can directly measure the host velocity dispersion from the AGN host spectra (e.g., Kauffmann et al. 2003; Heckman et al. 2004; Greene & Ho 2005a; Bian et al. 2006). The large number of quasars in the Sloan Digital Sky Survey (SDSS) make it possible to tackle the $M_{\text{BH}}-\sigma_*$ relation in radio-loud quasars (e.g. Bian & Zhao 2004; Salviander et al. 2007).

The dichotomy of radio loudness in quasars has been a persistent question since the discovery of quasars (Sandage 1965; Strittmatter et al. 1980; Kellermann et al. 1989). The radio luminosity is assumed to come from the relativistic electrons powered by a jet that is intimately connected with the SMBH (e.g., Begelman et al. 1984; Blundell & Beasley 1998). In the scale-free jet physics and accretion theories, the radio luminosity is related to the central engine parameters, such as the SMBH mass, SMBH spin, and Eddington ratio, etc. (Heinz & Sunyaev 2003). For radio-loud or radio-quiet quasars, a dependence of the radio loudness/luminosity on the SMBH mass/Eddington ratio has been argued for by some authors, and against by some others (e.g., Franceschini et al. 1998; Laor 2000; Lacy et al. 2001; Ho 2002; Woo & Urry 2002; McLure & Jarvis 2004; Wang et al. 2004; Greene et al. 2006; Liu et al. 2006; Sikora 2007; Panessa et al. 2007). Laor (2003) gave some comments on the origin of the AGN radio loudness and pointed out some error in the SMBH mass estimation for radio-loud AGNs in the literature, which is mainly due to the optical spectra with low signal-to-noise ratios, with no correction of the $\text{H}\beta$ contribution from the NLRs.

In this paper, we use a larger number of quasars with redshifts $z < 0.83$ in the SDSS Data Release 3 (DR3, see Abazajian et al. 2005) to investigate the $M_{\text{BH}}-\sigma_*$ relation and the dependence of the radio luminosity on the SMBH mass and the Eddington ratio for radio-loud and radio-quiet quasars. In Section 2, we show the SDSS quasars Data Release 3 catalog. Section 3 presents the data analysis. Section 4 shows the methods of calculating the SMBH masses and the Eddington ratios. Our results and discussion of the $M_{\text{BH}}-\sigma_*$ relation and the origin of radio luminosity are given in Sections 5 and 6, respectively. The last section lists our conclusions. All of the cosmological calculations in this paper assume $H_0 = 70 \text{ km s}^{-1} \text{ Mpc}^{-1}$, $\Omega_M = 0.3$, $\Omega_\Lambda = 0.7$.

2 SAMPLE AND DATA ANALYSIS

The sample used in this paper is selected from the SDSS quasars Catalog III, which covers a spectroscopic area of 1360 sq. deg., about 40% of the proposed SDSS survey area (Schneider et al. 2005). This catalog consists of 46,420 quasars in SDSS DR3 with $M_i < -22$. The catalog also contains radio emission properties from Faint Images of the Radio Sky at Twenty-cm (FIRST) survey within $2.0''$ of the quasars position (see col. (17) in their table 1).

The SDSS optical spectra cover the wavelength range 3800–9200 Å with a resolution of $1800 < R < 2100$. To calculate the SMBH mass from the broad $\text{H}\beta$ line and the host stellar velocity dispersion from the narrow $[\text{O III}]$ line, we shall consider a sample of 9753 quasars with redshifts less than 0.83. Because whether the SMBH mass from Mg II linewidth is consistent with that from $\text{H}\beta$ line width is still an open question (e.g., Salviander et al. 2007), so, here, we shall not consider using the Mg II linewidth to calculate the SMBH mass.

The radio luminosity at 5 GHz is calculated from the peak flux density listed in col. (17), table 2 in Schneider et al. (2005), for a spectral index of $\alpha = 0.5$, ($f_\nu \propto \nu^{-\alpha}$). The radio loudness R is calculated from: $R = f_{5\text{GHz}}/f_{\text{B}}$, where $f_{5\text{GHz}}$ and f_{B} are the rest-frame flux densities at 5 GHz and 4400 Å, with the k correction taken into consideration. $R = 10$ is commonly used to define radio-loud quasars and radio-quiet quasars (e.g., McLure & Jarvis 2004), as well as the radio luminosity at 5 GHz (e.g., Lacy 2001).

Of the 9573 quasars with $z < 0.83$ in SDSS DR3, 914 were detected by FIRST, 7846 were below the FIRST flux limit, and 993 quasars were not in the region covered by FIRST. For these objects not detected in FIRST, we only have upper-limits of the radio luminosity and the radio loudness. Of the quasars detected

in FIRST, 598 have $R \geq 10$, are classified as radio-loud and 316 have $R < 10$ are classified as radio-quiet. In addition, 5712 quasars not detected in FIRST and with $R < 10$ are classified as radio-quiet, and only with upper-limits of R and radio luminosity.

As we know, NLRs can contribute $H\beta$ emission to the total $H\beta$ profile; [O III] usually shows a non-symmetric profile and its narrow/core component can trace the stellar velocity better (e.g., Greene & Ho 2005a), the optical and ultraviolet Fe II multiples are often present in quasar spectra, and the Balmer continuum is required because of the existence of strong Balmer emission lines. Accordingly, we take following steps in our treatment of the SDSS spectral measurements.

- (1) We calculate the Galactic extinction in the observed spectra using the extinction law of Cardelli, Clayton & Mathis (1989) (IR band) and O'Donnell (1994) (optical band), then translate the spectra into the rest frame defined by the redshifts given in their FITS headers.
- (2) The optical and ultraviolet Fe II template from the prototype NLS1 I ZW 1 is used to subtract the Fe II emission from the spectra (Boroson & Green 1992; Vestergaard & Wilkes 2001). The I ZW 1 template is broadened by convolving it with a Gaussian of various linewidths and scaled by a multiplicative factor. A power-law continuum and Balmer continuum are added in the fitting. We calculate the Balmer continuum following Grandi (1982) and also add the high order Balmer lines at the red side of the Balmer edge using the result in Storey & Hummer (1995). The best subtraction of the Fe II, power-law and Balmer continuum is found when χ^2 is minimized in the fitting windows: 3550–3645, 4170–4260, 4430–4770, 5080–5550, 6050–6200 and 6890–7010 Å (see a sample fit in the top panel of Fig. 1). The monochromatic luminosity at 5100 Å ($\lambda L_\lambda(5100 \text{ \AA})$) is calculated from the power-law continuum.
- (3) Two sets of two-Gaussians are used to model the [O III] $\lambda\lambda 4959, 5007$ lines. A three-Gaussian is used to model the $H\beta$ line. For the doublet [O III] $\lambda\lambda 4959, 5007$, we take the same linewidth for each component, and fix the flux ratio of [O III] $\lambda 4959$ to [O III] $\lambda 5007$ at 1:3. Two components of $H\beta$ (supposed from NLRs) are set to have the same linewidth of each component of [O III] $\lambda 5007$ and their fluxes are constrained to be less than 1/2 of each of the components of [O III] $\lambda 5007$. The linewidth of the broad component of $H\beta$ is used to trace the virial velocity around the central SMBH (see a sample fit in the bottom panel of Fig. 1).

From the above spectral measurement, we obtain the full width at half maximum (FWHM) of the broad $H\beta$ line and the narrow/core [O III] line ($\text{FWHM}_{H\beta}$, $\text{FWHM}_{[\text{O III}]}$), the monochromatic luminosity at 5100 Å ($\lambda L_\lambda(5100 \text{ \AA})$), the total $H\beta$ luminosity ($L_{H\beta}$), as well as the radio luminosity and the radio loudness for the SDSS DR3 quasars with $z < 0.83$.

Objects without the $H\beta$ or [O III] lines are removed. In order to obtain reliable spectra fit, we carefully select objects for the analysis. The line equivalent width (EW) can show the line signal-to-noise ratios. The error of EW can be regarded as an indicator of the goodness of fit. Because the $H\beta$ line is usually strong, we do not constrain the EW of the $H\beta$ line, only constrain the error in the EW of the $H\beta$ line. We select objects by the criteria, EW of [O III], greater than 1.5, errors of the EWs of $H\beta$ and [O III] $\lambda\lambda 4959, 5007$, less than 100%. It led to 367 radio-loud quasars and 3677 radio-quiet quasars, including 207 radio-quiet quasars with measured radio luminosity. Then we visually checked these spectra one by one.

At last, we obtain a sample of 3772 quasars with a better multi-component model of $H\beta$ and [O III] lines, which includes 3466 radio-quiet quasars (hereafter “RQ total sample”), 306 radio-loud quasars (hereafter “RL sample”). Most objects in these 3466 radio-quiet quasars only have upper-limits of radio luminosity and radio loudness, but 181 radio-quiet quasars (hereafter “RQ sample”) have measured radio luminosities and radio loudnesses. We use the radio-quiet sample as the control sample to check the $M_{\text{BH}}-\sigma_*$ relation in radio-loud quasars.

3 SMBH MASS, EDDINGTON RATIO AND STELLAR VELOCITY DISPERSION

The size of the BLR is calculated from the monochromatic luminosity at 5100 Å ($\lambda L_\lambda(5100 \text{ \AA})$) or the $H\beta$ luminosity by the following formulae (Kaspi et al. 2005):

$$R_{\text{BLR}}^{\lambda L_\lambda(5100 \text{ \AA})} = (22.3 \pm 2.1) \left(\frac{\lambda L_\lambda(5100 \text{ \AA})}{10^{44} \text{ erg s}^{-1}} \right)^{0.69 \pm 0.05} \text{ lt - days}, \quad (1)$$

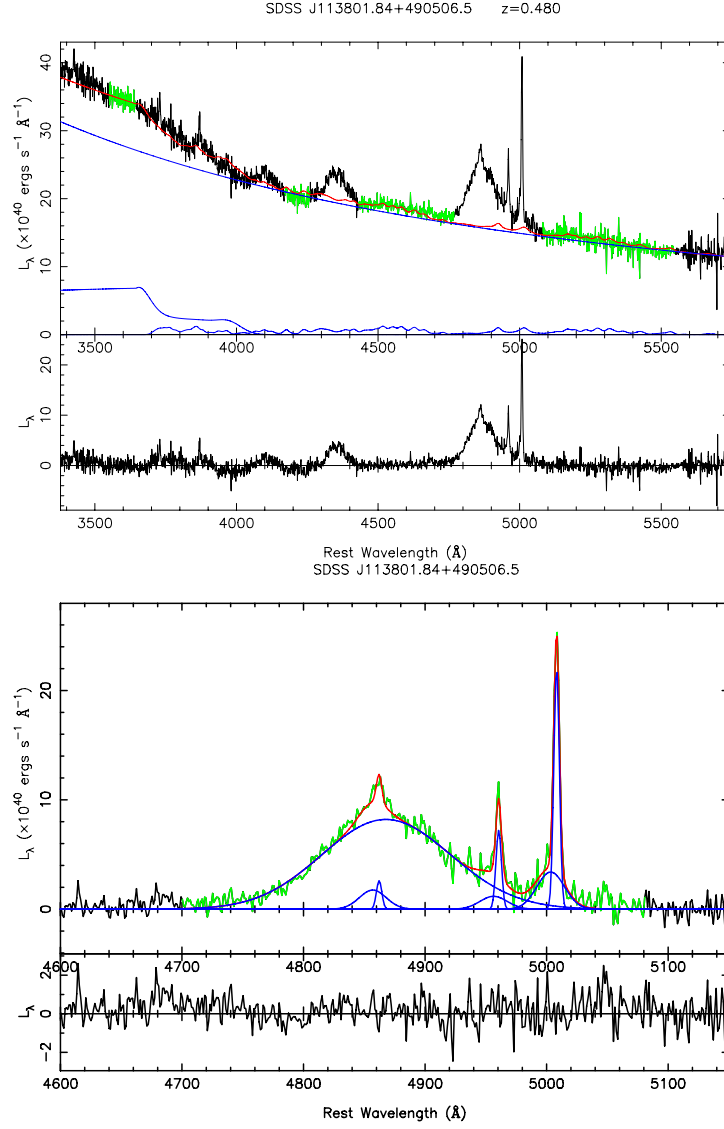


Fig. 1 Sample SDSS spectrum. SDSS J113801.84+490506.5. In the top panel, the black curve is the observed spectrum, the red line is the sum of the power-law the continuum, the Balmer continuum, and the Fe II multiples (blue curves). The green ranges are our fitting windows. The bottom panel is the multi-Gaussian fit for H β and [O III] lines. The red line is the sum of all multi-Gaussian (blue curves). The green curve is our fitting range of the pure H β and [O III] emissions after the subtraction of the power-law continuum, the Balmer continuum and Fe multiples.

$$R_{\text{BLR}}^{L_{\text{H}\beta}} = (82.3 \pm 7.0) \left(\frac{L_{\text{H}\beta}}{10^{43} \text{ erg s}^{-1}} \right)^{0.80 \pm 0.11} \text{ lt - days.} \quad (2)$$

We use the FWHM of the broad H β line (FWHM $_{\text{H}\beta}$) to trace the BLR's virial velocity: $v_{\text{BLR}} = \sqrt{f} \times \text{FWHM}_{\text{H}\beta}$, f being the calibration factor. If the BLR cloud is disk-like with a inclination of θ (Wills & Browne 1986), then we have

$$\text{FWHM}_{\text{H}\beta} = 2(v_r^2 + v_{\text{BLR}}^2 \sin^2 \theta)^{1/2}, \quad (3)$$

where v_r is the random isotropic component. We can then calculate the SMBH mass by $M_{\text{BH}} = \frac{R_{\text{BLR}} v_{\text{BLR}}^2}{G}$ (Kaspi et al. 2000; Kaspi et al. 2005):

$$M_{\text{BH}} = f \times 4.35 \times 10^6 \left(\frac{\text{FWHM}_{\text{H}\beta}}{10^3 \text{km s}^{-1}} \right)^2 \left(\frac{\lambda L_{\lambda}(5100 \text{ \AA})}{10^{44} \text{erg s}^{-1}} \right)^{0.69} M_{\odot}, \quad (4)$$

$$M_{\text{BH}} = f \times 1.61 \times 10^7 \left(\frac{\text{FWHM}_{\text{H}\beta}}{10^3 \text{km s}^{-1}} \right)^2 \left(\frac{L_{\text{H}\beta}}{10^{43} \text{erg s}^{-1}} \right)^{0.80} M_{\odot}. \quad (5)$$

Onken et al. (2004) did a calibration with the $M_{\text{BH}}-\sigma_*$ relation and suggested $f \approx 1.4$ (see also Collin et al. 2006; Dasyra et al. 2007). In our mass calculation, we adopt random orbits of BLR clouds and $f = 0.75$.

We calculate the Eddington ratio, i.e., the ratio of the bolometric luminosity (L_{bol}) to the Eddington luminosity (L_{Edd}), where $L_{\text{Edd}} = 1.26 \times 10^{38} (M_{\text{BH}}/M_{\odot}) \text{erg s}^{-1}$. The bolometric luminosity is calculated from the monochromatic luminosity at 5100 Å $L_{\text{bol}} = c_{\text{B}} \lambda L_{\lambda}(5100 \text{ \AA})$, with an adopted correction factor c_{B} of 9 (Kaspi et al. 2000; Marconi et al. 2004; Richards et al. 2006; Netzer & Trakhtenbrot 2007).

We use the gas velocity dispersion of the narrow/core [O III] component from the NLRs to trace the host stellar velocity dispersion, $\sigma_{[\text{OIII}]}^n = \sqrt{\sigma_{\text{obs}}^2 - [\sigma_{\text{inst}}/(1+z)]^2}$, where $\sigma_{\text{obs}} = \text{FWHM}_{[\text{OIII}]}^n/2.35$, z is the redshift (Bian et al. 2006). For the SDSS spectra, the mean value of the instrumental resolution, σ_{inst} , is 60 km s⁻¹ for [O III] (e.g. Greene & Ho 2005a).

In Figure 2, we present number distributions of the SMBH mass, $\lambda L_{\lambda}(5100 \text{ \AA})$ and $\text{FWHM}_{\text{H}\beta}$, $\sigma_{[\text{OIII}]}^n$ for 181 radio-quiet quasars (top), 306 radio-loud quasars with measured radio luminosity (middle), and 3466 radio-quiet quasars (bottom). The mean of SMBH mass is 8.65 ± 0.03 (s.d.= 0.45) for the RL sample, 8.36 ± 0.04 (s.d.=0.48) for the RQ sample with reliable radio luminosity, and 8.32 ± 0.01 (s.d.= 0.43) for the ‘‘total’’ RQ sample. The radio-loud quasars have larger SMBH masses, and only a few have masses less than $10^8 M_{\odot}$ (see Fig. 3). This is consistent with the results of McLure & Jarvis (2004). They also have smaller Eddington ratios than the radio-quiet quasars (see Table 1). We find that, for radio-loud quasars, the mean of H β FWHM is $7493 \pm 165 \text{ km s}^{-1}$ (s.d.=2882 km s⁻¹), the mean of $\log \lambda L_{\lambda}(5100 \text{ \AA})$ is $44.86 \pm 0.03 \text{ erg s}^{-1}$ (s.d.= 0.45); for radio-quiet quasars, the mean of H β FWHM is $5780 \pm 176 \text{ km s}^{-1}$ (s.d.= 2389 km s⁻¹); the mean of $\log \lambda L_{\lambda}(5100 \text{ \AA})$ is $44.81 \pm 0.01 \text{ erg s}^{-1}$ (s.d.= 0.46). Radio-loud quasars tend to have larger H β FWHM and $\lambda L_{\lambda}(5100 \text{ \AA})$, hence larger SMBH masses (Sulentic et al. 2000).

4 THE $M_{\text{BH}}-\sigma_*$ RELATION

4.1 The Mass Deviation from the $M_{\text{BH}}-\sigma_*$ Relation

In Figure 3, we show $M_{\text{BH}}-\sigma_*$ relation for radio-loud and radio-quiet quasars. The solid line in Figure 3 is the $M_{\text{BH}}-\sigma_*$ relation for normal nearby galaxies given by Tremaine et al. (2002), $M_{\text{BH}}(\sigma_*) = 10^{8.13} [\sigma_*/(200 \text{ km s}^{-1})]^{4.02} M_{\odot}$. In both left and right panels of Figure 3, $\lambda L_{\lambda}(5100 \text{ \AA})$ and $L_{\text{H}\beta}$ are respectively used to calculate the SMBH mass. In Figure 3, the correlation between M_{BH} and $\sigma_{[\text{OIII}]}^n$ is very weak for the larger sample of SDSS quasars. It is possibly due to the accuracy of the stellar velocity dispersion derived from the narrow/core [O III] line-width. However, it is obvious that the sample of radio-loud quasars deviated more from the solid line than the sample of radio-quiet quasars. This is consistent with our previous results (Bian & Zhao 2004).

We calculate the black hole mass deviation $\Delta \log M_{\text{BH}}$ from the solid line defined by Tremaine et al. (2002), $\Delta \log M_{\text{BH}} = \log M_{\text{BH}}(\text{H}\beta) - \log M_{\text{BH}}(\sigma_*)$, where σ_* is defined to be $\sigma_{[\text{OIII}]}^n$. For the mass derived from $\lambda L_{\lambda}(5100 \text{ \AA})$, the mean of $\Delta \log M_{\text{BH}}$ is 0.65 ± 0.04 with a standard deviation of 0.71 for the RL sample of 306 radio-loud quasars, 0.04 ± 0.04 with a standard deviation of 0.63 for the RQ sample of 181 radio-quiet quasars with reliable radio luminosities, and 0.14 ± 0.01 with a standard deviation of 0.62 for total radio-quiet sample of 3466 quasars. We find that they are almost the same as in the case of the mass derived from $L_{\text{H}\beta}$. In the following analysis, we shall just consider the masses and Eddington ratios calculated from $\lambda L_{\lambda}(5100 \text{ \AA})$.

In the top panel of Figure 4, we plot the deviation of the SMBH mass from the $M_{\text{BH}}-\sigma_*$ relation versus the radio loudness. It is obvious that the deviation increases with increasing radio loudness. In the bottom panel of Figure 4, we plot the deviation of the SMBH mass from the $M_{\text{BH}}-\sigma_*$ relation versus

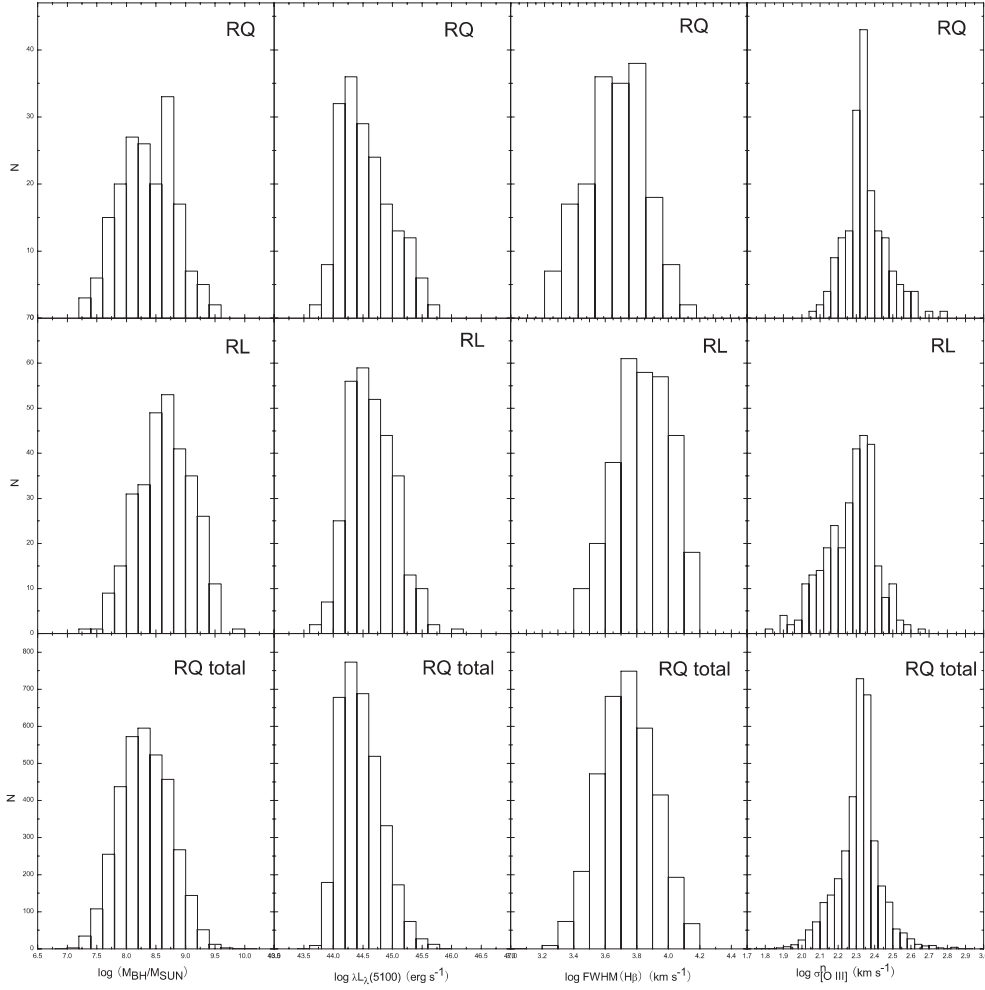


Fig. 2 Number distributions of M_{BH} , $\lambda L_{\lambda}(5100 \text{ \AA})$ and $\text{FWHM}_{\text{H}\beta}$, $\sigma_{[\text{OIII}]}$ for 181 radio-quiet quasars (top row), 306 radio-loud quasars with measured radio luminosity (middle row), and 3466 radio-quiet quasars (“the total RQ sample”, bottom row).

the redshift. We find a weak correlation for radio-quiet quasars. A simple least-square regression gives: $\Delta \log M_{\text{BH}} = (1.00 \pm 0.06)z - (0.29 \pm 0.03)$. The correlation coefficient R is 0.26, with a probability of $p_{\text{null}} < 10^{-4}$ for the null hypothesis of no correlation. In Figure 5, we show the redshift distributions for the radio-quiet and radio-loud quasars. The radio-loud quasars (red circles) have larger redshifts than the radio-quiet quasars (blue stars) (see Fig. 5).

In Table 1, we show the mean values of the masses and Eddington ratios in different redshift bins for the different samples.

4.2 Uncertainties

There are some factors leading to the uncertainty in the calculated SMBH mass: the uncertainties of $\text{H}\beta$, $[\text{O III}]$ line width, $\lambda L_{\lambda}(5100 \text{ \AA})$ and $L_{\text{H}\beta}$ when the multi-components are used to model the SDSS spectra, and the systematic errors in Equations (1)–(5) from the uncertainties of the BLRs geometry and dynamics. The uncertainty of our calculated SMBH mass is about 0.5 dex, while the uncertainty of the Eddington ratio is about 0.5 dex or greater. For the radio-loud quasars, we should note two effects: the relativistic beaming effect on the optical continuum and the orientation of the BLRs. The total $\text{H}\beta$ luminosity instead

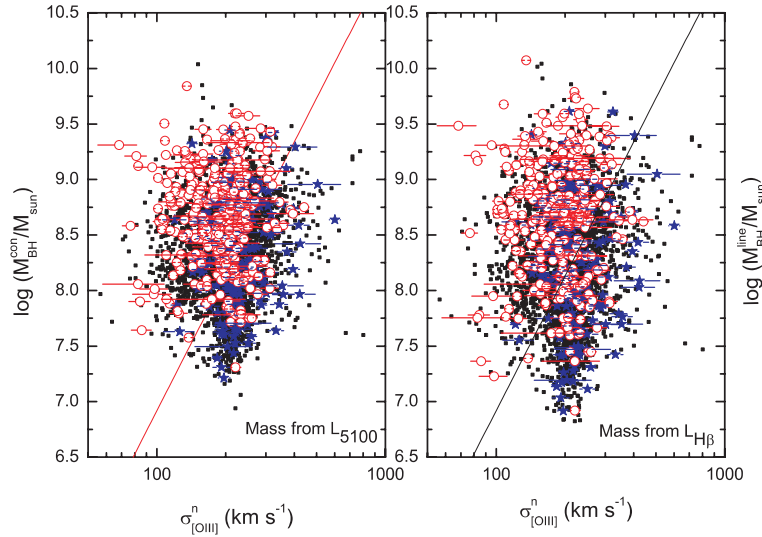


Fig. 3 $M_{\text{BH}}-\sigma_*$ relation for radio-loud and radio-quiet quasars. Red circles denote radio-loud quasars, blue stars denote radio-quiet quasars with measured radio luminosities, black squares denote radio-quiet quasars with upper-limits of radio luminosity. The mass in the left panel is derived from $\lambda L_{\lambda}(5100 \text{ \AA})$, and the mass in the right panel is derived from $H\beta$ luminosity.

Table 1 Mean quantities in different redshift bins for the different samples. L_{cut} is calculated from the QSOs luminosity function (Boyle et al. 2000) to make the mean luminosity of the kept QSOs ($L > L_{\text{cut}}$) equal to the observed mean luminosity in different redshift bins. $L_0 = 0.3L_{\text{Edd}}(M_{\text{gal}}^*)$, where $M_{\text{gal}}^* = 10^{11} M_{\odot}$ in the galaxy mass function $\Phi(M_{\text{gal}}) = \Phi^*(M_{\text{gal}}/M_{\text{gal}}^*)^{-\alpha} e^{-M_{\text{gal}}/M_{\text{gal}}^*}$ (Drory et al. 2005).

z	N	$\log(\lambda L_{\lambda}(5100 \text{ \AA}) \text{ erg s}^{-1})$	$\log(M_{\text{BH}}/M_{\odot})$	$\log(L_{\text{Bol}}/L_{\text{Edd}})$	$\Delta \log M_{\text{BH}}$	$\log L_{\text{cut}}/L_0$	$\Delta \log M_{\text{BH}}^{\text{simu}}$
(1)	(2)	(3)	(4)	(5)	(6)	(7)	(8)
RQ Total							
0.1–0.2	198	44.08 ± 0.17	7.81 ± 0.41	-1.05 ± 0.40	-0.08 ± 0.54	-1.38	0.04
0.2–0.3	586	44.17 ± 0.21	7.92 ± 0.39	-1.06 ± 0.37	-0.02 ± 0.61	-1.30	0.06
0.3–0.4	824	44.32 ± 0.24	8.05 ± 0.43	-1.02 ± 0.36	0.07 ± 0.58	-1.18	0.09
0.4–0.5	745	44.48 ± 0.22	8.24 ± 0.41	-0.98 ± 0.36	0.08 ± 0.61	-0.98	0.15
0.5–0.6	518	44.67 ± 0.24	8.49 ± 0.43	-0.97 ± 0.37	0.30 ± 0.61	-0.74	0.21
0.6–0.7	327	44.82 ± 0.23	8.62 ± 0.43	-0.93 ± 0.33	0.37 ± 0.60	-0.58	0.24
0.7–0.83	267	45.04 ± 0.23	8.80 ± 0.39	-0.87 ± 0.34	0.41 ± 0.63	-0.38	0.26
RQ							
0.1–0.4	114	44.35 ± 0.32	8.21 ± 0.32	-1.01 ± 0.39	-0.04 ± 0.63	-1.14	0.10
0.4–0.82	67	44.94 ± 0.34	8.62 ± 0.41	-0.83 ± 0.32	0.17 ± 0.61	-0.50	0.25
RL							
0.1–0.3	35	44.25 ± 0.29	8.25 ± 0.38	-1.15 ± 0.42	0.01 ± 0.68	-1.22	0.08
0.3–0.5	109	44.49 ± 0.31	8.51 ± 0.45	-1.17 ± 0.39	0.52 ± 0.80	-0.98	0.15
0.5–0.7	106	44.78 ± 0.35	8.78 ± 0.38	-1.14 ± 0.32	0.80 ± 0.63	-0.66	0.23
0.7–0.83	56	44.98 ± 0.29	8.91 ± 0.39	-1.08 ± 0.33	0.95 ± 0.75	-0.46	0.26

of $\lambda L_{\lambda}(5100 \text{ \AA})$ is used to account for the first effect. We find the effect is small in our sample, and there is no correlation between the $H\beta$ EW and the radio loudness (e.g. Wu et al. 2004). Lacy et al. (2001) made a small correction for the orientation of BLRs by a factor of $R_c^{0.1}$, where R_c is the ratio of the core to extended radio luminosity. They adopted $R_c = 0.1$ for steep-spectrum quasars and $R_c = 10$ for flat-spectrum quasars in the absence of measured R_c . This will lead to an uncertainty of about 0.2 dex in $\Delta \log M_{\text{BH}}$.

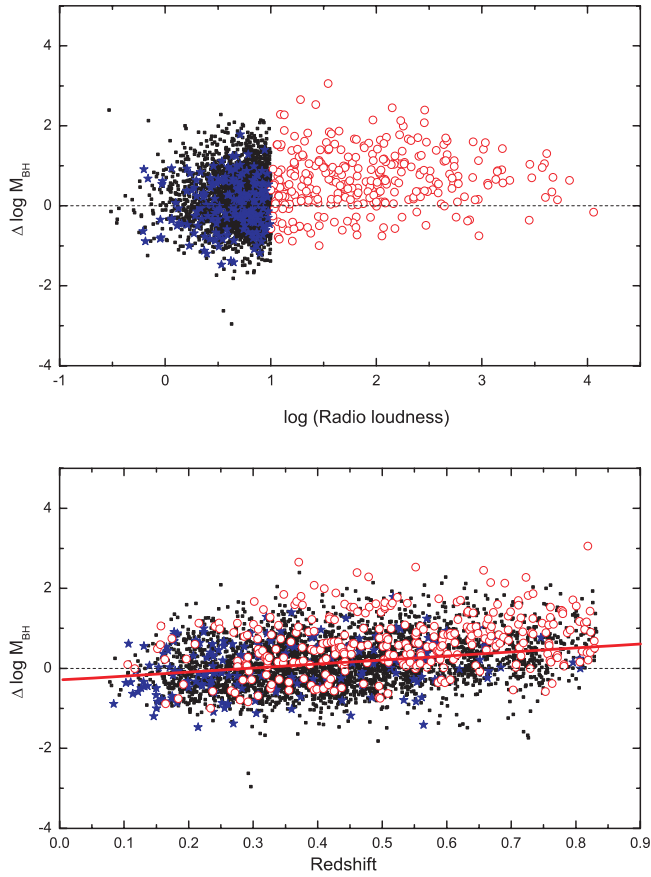


Fig. 4 Top: Deviation of the SMBH mass from the Tremaine’s $M_{\text{BH}}-\sigma_*$ relation in Fig. 2 versus the radio loudness. The dash line denotes $\Delta \log M_{\text{BH}} = 0$. Bottom: Deviation of the SMBH mass from the Tremaine’s $M_{\text{BH}}-\sigma_*$ relation in Fig. 2 versus the redshift. The red solid line denotes our best fit for all radio-quiet quasars. Symbols are as same as in Fig. 3.

The fiber in the SDSS spectroscopic survey has a diameter of $3''$ on the sky. The SDSS spectra of lower-redshift quasars possibly have obvious stellar light contribution, which can be used to directly measure the stellar velocity dispersion (e.g., Kauffmann et al. 2003; Heckman et al. 2004; Bian et al. 2006). For luminous quasars ($M_i < -22$), the stellar light contribution can be omitted or has little effect on the mass calculation (e.g., Van den Berk et al. 2006).

It is possible that jets can have a dynamical effect on the NLRs and may have a systematically different effect on the [O III] profile (Nelson & Whittle 1996). However, when the [O III] profile broadening by jets is considered, the correction of the [O III] gas velocity dispersion will lead the radio-loud quasars to deviate much more from the $M_{\text{BH}} - \sigma_*$ relation.

We select quasars with EW of narrow [O III] component greater than 1.5, and EW errors of $\text{H}\beta$ and [O III] $\lambda\lambda 4959, 5007$ less than 100%. Different criteria would lead to different numbers of quasars (such as error of EWs less than 5%, 50%, or 100%, $\chi^2 < 4$). However, we find that the main results do not change.

4.3 The Mass Deviation from the Luminosity Bias

Salviander et al. (2007) also used SDSS DR3 quasars to explore the cosmological evolution of the $M_{\text{BH}}-\sigma_*$ relation. After a careful consideration of the selection biases and intrinsic scatter in the $M_{\text{BH}}-\sigma_*$ relation, they suggested that the $M_{\text{BH}}-\sigma_*$ relation appears to evolve with redshift. Netzer & Trakhtenbrot (2007)

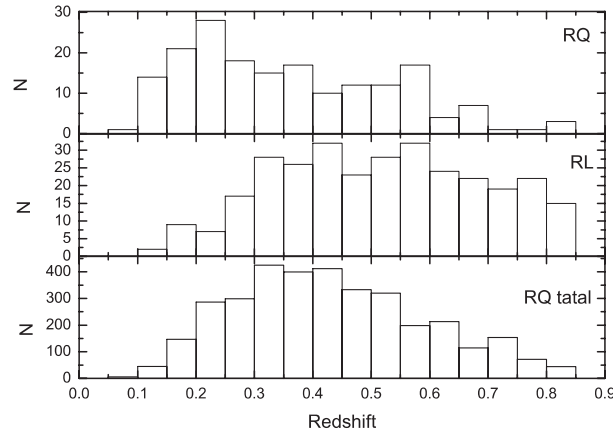


Fig. 5 Redshift distributions for 181 radio-quiet quasars with radio loudness (top), 306 radio-loud quasars with measured radio luminosity (middle), and the total radio-quiet sample of 3466 quasars (bottom).

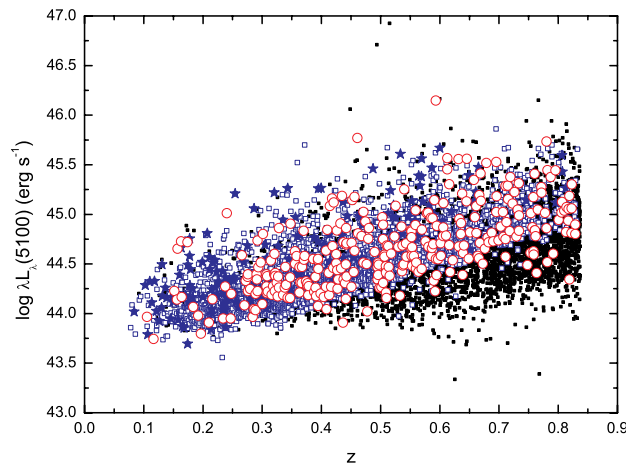


Fig. 6 $\lambda L_{\lambda}(5100 \text{ \AA})$ versus z . Open circles denote RL sample, blue stars denote RQ, QSOs with measured radio loudness, blue squares denote RQ QSOs with upper-limits of radio loudness, and small black squares denote all 9753 SDSS DR3 QSOs with $z < 0.83$. Some faint objects are missed in our selection.

also found a nonlinear $M_{\text{BH}}-\sigma_*$ relation with different slopes for different redshift bins. In our sample selection, the line fitting favored brighter objects (i.e. luminosity bias, see Fig. 6). Following Salviander et al. (2007), we calculate the contribution of $\Delta \log M_{\text{BH}}$ from this luminosity bias. We calculate the mean observed luminosity in different redshift bins for our different samples (i.e. RQ total sample; RQ sample; RL sample). Using the QSOs luminosity function (Boyle et al. 2000), we calculate the cut luminosity to make the mean luminosity of the kept QSOs ($L > L_{\text{cut}}$) equal to the observed mean luminosity in different redshift bin. Then we carry out simulations to calculate the contribution of $\Delta \log M_{\text{BH}}$ from this luminosity bias (for detail in Salviander et al. 2007). We obtain a formula: $\Delta \log M_{\text{BH}}^{\text{simu}} = 0.292 + 0.1138x + 0.265x^2 + 0.480x^3 + 0.182x^4$, where x is $\log(L_{\text{cut}}/L_0)$, $L_0 = 0.3L_{\text{Edd}}(M_{\text{gal}}^*)$, $M_{\text{gal}}^* = 10^{11}M_{\odot}$ (Drory et al. 2005). We find that the mass deviation from the luminosity bias monotonically increases with increasing redshift (see col. (8) in Table 2). Table 1 shows our results. Here, col. (1) is the given redshift bin, col. (2) the number in the given bin, cols. (3)–(5) the mean values of 5100 Å luminosity, mass, and Eddington ratio. Col. (6) shows the mean mass deviation from the $M_{\text{BH}}-\sigma_*$ relation, col. (7), $\log(L_{\text{cut}}/L_0)$, and col. (8) our simulated mass deviation for different cut luminosities in different redshift bins.

Table 2 Mean quantities in different redshift bins. Here a, b_1, b_2 is defined by $\log L_{5\text{GHz}} = a + b_1 \log M_{\text{BH}} + b_2 \log(L_{\text{Bol}}/L_{\text{Edd}})$. For different samples, the first line is for the result by χ^2 minimization, and in the second line, quantities in brackets are the mean values of a, b_1, b_2 by ASURV, the last three lines are results accounting different dependent variables by ASURV.

Dependent variable (1)	a (2)	b_1 (3)	b_2 (4)	R -square (5)
RQ	$30.9^{+1.20}_{-1.80}$ (30.84 ± 2.21)	$1.28^{+0.23}_{-0.16}$ (1.27 ± 0.29)	$1.29^{+0.31}_{-0.24}$ (1.26 ± 0.53)	
$L_{5\text{GHz}}$	33.18 ± 0.43	0.95 ± 0.05	0.81 ± 0.07	0.64
M_{BH}	28.79 ± 1.54	1.52 ± 0.02	1.12 ± 0.08	0.72
$L_{\text{Bol}}/L_{\text{Edd}}$	30.54 ± 3.04	1.35 ± 0.09	1.85 ± 0.02	0.57
RL	$19.7^{+5.40}_{-3.90}$ (22.43 ± 10.4)	$3.10^{+0.60}_{-0.70}$ (2.68 ± 1.30)	$4.18^{+1.40}_{-1.10}$ (3.29 ± 1.94)	
$L_{5\text{GHz}}$	32.62 ± 0.82	1.24 ± 0.10	1.38 ± 0.13	0.35
M_{BH}	11.77 ± 3.54	3.85 ± 0.40	3.23 ± 0.19	0.53
$L_{\text{Bol}}/L_{\text{Edd}}$	22.89 ± 3.79	2.95 ± 0.16	5.26 ± 0.05	0.49
RL+RQ	$10.0^{+8.70}_{-4.20}$ (15.65 ± 12.93)	$4.30^{+0.70}_{-0.80}$ (3.46 ± 1.81)	$5.15^{+2.32}_{-1.69}$ (4.11 ± 3.81)	
$L_{5\text{GHz}}$	30.45 ± 0.73	1.38 ± 0.09	0.92 ± 0.12	0.31
M_{BH}	6.57 ± 2.74	4.34 ± 0.04	3.09 ± 0.17	0.53
$L_{\text{Bol}}/L_{\text{Edd}}$	9.92 ± 4.67	4.67 ± 0.25	8.33 ± 0.08	0.40

For the total RQ sample, the luminosity bias can explain most of the $\Delta \log M_{\text{BH}}$. For the highest redshift bin of $0.7 < z < 0.83$, $\Delta \log M_{\text{BH}}$ is about 0.15 dex after correcting for the luminosity bias. Possibly 0.15 dex in this highest redshift bin is due to cosmological evolution, which is consistent well with the result of Salvander et al. (2007). However, we should note that the standard deviation of $\Delta \log M_{\text{BH}}$ in different bins is about 0.6 dex, much greater than 0.15 dex. For the RQ sample, the observed $\Delta \log M_{\text{BH}}$ can be entirely contributed by the luminosity bias, which is possibly due to the smaller numbers in this sample. Therefore, we think there is no obvious deviation from the $M_{\text{BH}} - \sigma_*$ relation when the M_{BH} uncertainties and the luminosity bias are taken into consideration.

For the RL sample, after the contribution by the luminosity bias is corrected, $\Delta \log M_{\text{BH}}$ is still large (about 0.69 dex in $0.7 < z < 0.83$), and there is a trend that $\Delta \log M_{\text{BH}}$ gets larger with larger redshifts. After allowing for the possible $M_{\text{BH}} - \sigma_*$ cosmological evolution (0.15 dex in $0.7 < z < 0.83$), there is still a 0.54 dex deviation in $0.7 < z < 0.83$ for the radio loud QSOs. Bonning et al. (2005) suggested that narrower [O III] for radio loud quasars is responsible for this deviation from the $M_{\text{BH}} - \sigma_*$ relation, rather than the effect involving M_{BH} , but the cause of the deviation is rather unclear.

5 ORIGIN OF RADIO LUMINOSITY

5.1 $L_{5\text{GHz}} - L_{[\text{O III}]}$ Relation

The relation between the radio luminosity and the optical/X-ray luminosity, which provides the connection between the jet and accretion power, has been investigated by many groups (e.g. Xu et al. 1999; Ho 2002; Wang et al. 2004; Panessa et al. 2007; Sikora 2007). In Figure 7, we show the radio luminosity at 5 GHz versus the total [O III] luminosity. These two luminosities are all related to the redshift. By the partial Kendall's τ correlation test, we make a partial correlation analysis with redshift as the test variable (Akritas & Siebert 1996). For the RQ sample of 181 radio-quiet quasars, the partial Kendall's τ correlation is 0.237, with variance 0.0304, and the probability of null hypothesis 6.3×10^{-15} . For the RL sample of 306 radio-loud quasars, the τ correlation is 0.251, variance is 0.0456, and the probability of null hypothesis is 3.7×10^{-8} . We use the bivariate correlated errors and intrinsic scatter (BCES) regression method¹ of Akritas & Bershadsky (1996) (see also Isobe et al. 1990) to find the relation between $L_{[\text{O III}]}$ and $L_{5\text{GHz}}$, and adopt the BCES bisector result (e.g. Kaspi et al. 2005). For the RQ sample of 181 radio-quiet quasars with measured

¹ This is not the symmetric regression used by Merloni et al. (2003). For details see Section 5.2

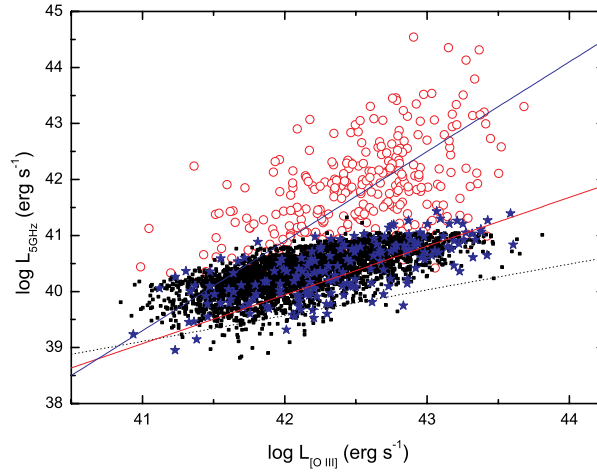


Fig. 7 Radio luminosity versus the [O III] luminosity. Red circles are radio-loud quasars, blue stars are radio-quiet quasars with measured radio luminosities, black squares are radio-quiet quasars with upper-limits of radio luminosity. The red solid line is the BCES bisector result for the radio-quiet quasars (blue stars). The blue solid line is the BCES bisector result for the radio-loud quasars (red circles). The dash line is the best fit for radio-quiet AGNs found by Xu et al. (1999).

radio luminosities, the BCES bisector result is, $\log L_{5\text{ GHz}} = (0.87 \pm 0.04)\log L_{[\text{O III}]} + (3.40 \pm 1.87)$ (red dash line in Fig. 7). For the RL sample of 306 radio-loud quasars, $\log L_{5\text{ GHz}} = (1.60 \pm 0.08)\log L_{[\text{O III}]} - (26.30 \pm 3.39)$.

Considering the errors of the intercept, our best fits for radio-quiet quasars in Figure 7 are consistent with the result found by Xu et al. (1999) (also see Ho & Peng 2001): $\log L_{5\text{ GHz}} = (0.45 \pm 0.07)\log L_{[\text{O III}]} + (20.25 \pm 0.6)$ (black dot line in Fig. 7). In the plot of the radio luminosity versus the optical/X-ray nuclear luminosity, the separation of radio-loud and radio-quiet quasars from SDSS DR3 is not so clear as in the other results (Xu et al. 1999; Terashima & Wilson 2003; Sikora et al. 2007). The difference is possibly due to the selection effect in the different wavelength bands.

The [O III] luminosity is usually assumed to be proportional to the accretion rate and this correlation can be explained in a model of accelerated and collimated jet by magnetic field (Xu et al. 1999). Apart from the dependence on the accretion rate, the radio luminosity is possibly dependent on such properties as mass or spin of the central SMBH (see e.g., Sikora et al. 2007 and refs. therein).

If we use the tight correlation between X-ray luminosity and [O III] luminosity (Xu et al. 1999), $\log L_x = 1.01\log L_{[\text{O III}]} + 1.6$, the relation between $L_{5\text{ GHz}}$ and $L_{[\text{O III}]}$ can be transformed to a relation between $L_{5\text{ GHz}}$ and L_x : $L_{5\text{ GHz}} \propto L_x^{0.86 \pm 0.06}$ for the RQ sample and $L_{5\text{ GHz}} \propto L_x^{1.58 \pm 0.10}$ for the RL sample. There exists an obvious difference in the slope between the radio-quiet and radio-loud quasars. For low luminosity AGNs, Panessa et al. (2007) suggested a correlation, $L_x \propto L_{5\text{ GHz}}^{0.97}$, and their index is between our two values for radio-quiet and radio-loud quasars. If we use the correlation suggested by Netzer et al. (2006), $L_{\text{O III}} \propto L_x^{0.704 \pm 0.06}$, the relation we found between $L_{5\text{ GHz}}$ and $L_{[\text{O III}]}$ can be transformed to $L_{5\text{ GHz}} \propto L_x^{0.61 \pm 0.04}$ for the RQ sample and to $L_{5\text{ GHz}} \propto L_x^{1.11 \pm 0.07}$ for the RL sample. The radio luminosity is often assumed to come from relativistic electrons powered by a jet. The result of the RL sample is consistent with that of Panessa et al. (2007). The X-ray emission is often assumed coming from both the accretion flow and the relativistic jet, being dominated by the accretion flow at high accretion rate, and by the jet emission at low accretion rate (Gallo et al. 2003; Yuan & Cui 2005). The relation between $L_{5\text{ GHz}}$ and L_x in different accretion rates can be explained by the jet-dominated X-ray models (Fender et al. 2003; Gallo et al. 2003; Heinz 2004; Yuan & Cui 2005).

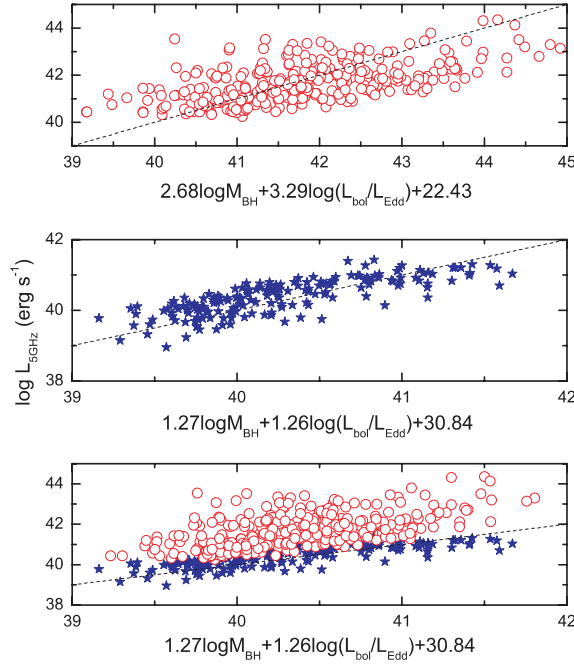


Fig. 8 Dependent of radio luminosity on the SMBH mass and the Eddington ratio. The indexes are adopted from the mean values in brackets in Table 1. Top panel is for radio-loud quasars, middle for radio-quiet quasars with measured radio luminosities, and bottom for them all. Symbols are as same as in Fig. 7. The dash lines are the 1:1 lines.

5.2 Dependence of Radio Luminosity on the SMBH Mass and Eddington Ratio

It has been suggested that the radio luminosity/radio loudness is related to the SMBH mass (e.g., Laor 2000). We calculate the dependence of the radio luminosity on the SMBH mass and the Eddington ratio in the form, $\log L_{5\text{GHz}} = a + b_1 \log M_{\text{BH}} + b_2 \log(L_{\text{Bol}}/L_{\text{Edd}})$ (see Fig. 8).

We first operate the multiple regression with ASURV Rev 1.2 (LaValley, Isobe & Feigelson 1992 and refs. therein) for the RQ sample, the RL sample and the RL+RQ sample. In order to avoid non-symmetric regression, we adopt the mean values of a , b_1 and b_2 when we use different independent variables in the multiple regressions (see col. (1) in Table 1). In all the multiple regressions, the probability for the null hypothesis of no correlation being true is $p_{\text{null}} < 10^{-4}$. The R-Square correlation coefficient for the RQ sample is larger than for the other two samples (see Table 2, Fig. 8).

We also carry out the symmetric multivariate regression analysis, with $y = a + b_1 x_1 + b_2 x_2$, directly by the χ^2 estimator, $\chi^2 = \sum_i \frac{(y_i - a - b_1 x_{1i} + b_2 x_{2i})^2}{\sigma_{y_i}^2 + (b_1 \sigma_{x_{1i}})^2 + (b_2 \sigma_{x_{2i}})^2}$ (Press et al. 1992; Tremaine et al. 2002; Merloni et al. 2003), σ being the corresponding uncertainties. Considering the same uncertainties (σ) of radio luminosity, mass and the Eddington ratio (Tremaine et al. 2002; Merloni et al. 2003), we re-normalize these uncertainties to make the minimum χ^2/n_{dof} unity. The results are listed in the first line for a given sample in Table 1.

Considering the errors of a , b_1 and b_2 in Table 2, the results from ASURV and χ^2 agree very well. Therefore, in the next analysis, we adopt the values of a , b_1 and b_2 from the χ^2 estimation (Table 1), i.e. $L_{5\text{GHz}} \propto M_{\text{BH}}^{1.28^{+0.23}_{-0.16}} (L_{\text{Bol}}/L_{\text{Edd}})^{1.29^{+0.31}_{-0.24}}$ for the RQ sample, $L_{5\text{GHz}} \propto M_{\text{BH}}^{3.10^{+0.60}_{-0.70}} (L_{\text{Bol}}/L_{\text{Edd}})^{4.18^{+1.40}_{-1.10}}$ for the RL sample, and $L_{5\text{GHz}} \propto M_{\text{BH}}^{4.30^{+0.70}_{-0.80}} (L_{\text{Bol}}/L_{\text{Edd}})^{5.15^{+2.32}_{-1.69}}$ for the RL+RQ sample.

Ho (2002) suggested a correlation between the nucleus radio loudness and the Eddington ratio (Gallo et al. 2003; Greene et al. 2006; Sikora et al. 2007; Panessa et al. 2007). We also use the multiple regression by ASURV to search the dependence of the radio loudness on the SMBH mass and the Eddington ratio

(with radio luminosity as the dependent variable). However, the R-Square correlation coefficient is very low for the RL sample and the RQ sample. For the RL+RQ sample, we find a weak correlation between the radio loudness and the SMBH mass (the simple least-square correlation coefficient $R = 0.26$), and a much weaker correlation between the radio loudness and the Eddington ratio ($R = -0.15$). The range of the Eddington ratio is between 0.01 to 1 for our RL sample and RQ sample. Moreover, our sample is composed of broad-line type-I quasars, which just fill the gap between two sequences in the plot of radio loudness versus the Eddington ratio (see fig. 3 in Sikora et al. 2007). Considering the disk-jet connection model, the X-ray luminosity might be a better tracer of SMBHs accretion power than the optical luminosity (Panessa et al. 2007). We also should pay more attention to narrow-line Seyfert 1 galaxies with larger Eddington ratios in this plot (Zhou & Wang 2002; Whalen et al. 2006; Komossa et al. 2006).

For scale-free jet physics, Heinz & Sunyaev (2003) derived the dependence of the accretion-powered jets flux (f_v) on the SMBH mass and the dimensionless accretion rates for different accretion scenarios (see their table 1). For the radiation-pressure-supported standard accretion disk, $f_v \propto M_{\text{BH}}^{17/12-\alpha/3}$; for the gas-pressure-supported standard accretion disk, $f_v \propto M_{\text{BH}}^{(187-32\alpha)/120} \dot{m}^{(17/12+2\alpha/3)4/5}$; and for ADAF, $f_v \propto M_{\text{BH}}^{17/12-\alpha/3} \dot{m}^{17/12+2\alpha/3}$, α being the radio spectral index. Assuming $\alpha = 0.5$, for the radiation-pressure-supported standard accretion disk, $f_v \propto M_{\text{BH}}^{1.25}$; for the gas-pressure-supported standard accretion disk, $f_v \propto M_{\text{BH}}^{1.43} \dot{m}^{1.40}$; and for ADAF, $f_v \propto M_{\text{BH}}^{1.25} \dot{m}^{1.75}$. Regarding the large scatter in b_1 and b_2 , our results are consistent with the above radio origin of scale-free jet model. However, by our data we cannot distinguish the different disks for radio-quiet and radio-loud quasars in this accretion-powered jet model.

6 CONCLUSIONS

Taking advantage of the large number of quasars in the SDSS DR3 catalog, we use a multi-component model to model the SDSS spectra and calculate the SMBH masses. Combined with the radio properties from FIRST, we obtain a sample of 3772 quasars with reliable SMBH masses, including 306 radio-loud quasars, 3466 radio-quiet quasars with measured radio luminosity or upper-limit of radio luminosity (181 radio-quiet quasars have measured radio luminosity). Two main results are suggested: (1) The deviation from the $M_{\text{BH}} - \sigma_*$ relation of the nearby normal galaxies given by Tremaine et al. (2002) is much greater in the radio-loud quasars than in the radio-quiet quasars. This is partly due to a possible cosmological evolution of the $M_{\text{BH}} - \sigma_*$ relation and to the luminosity bias. (2) The radio luminosity is correlated with the central SMBH mass and the Eddington ratio, $\propto M_{\text{BH}}^{1.28^{+0.23}_{-0.16}} (L_{\text{Bol}}/L_{\text{Edd}})^{1.29^{+0.31}_{-0.24}}$ for radio-quiet quasars and $\propto M_{\text{BH}}^{3.10^{+0.60}_{-0.70}} (L_{\text{Bol}}/L_{\text{Edd}})^{4.18^{+1.40}_{-1.10}}$ for radio-loud quasars. The weaker correlation of radio luminosity with mass and the Eddington ratio in the radio-loud quasars shows that other physical factors must impact on the radio luminosity, such as the SMBH spin.

Acknowledgements We thank Luis C. Ho for his very helpful comments. We thank Dr. M. Wu and Z. H. Fan for helpful discussions. We thank the anonymous referee for his/her comments and instructive suggestions. This work has been supported by the NSFC (Nos. 10403005, 10473005, 10873010 and 10733010), National Basic Research Program of China (No. 2009CB824800), the Science-Technology Key Foundation from Education Department of China (No. 206053), and China Postdoctoral Science Foundation (No. 20060400502). Chen Hu thanks T. A. Boroson & M. Vestergaard for the I ZW 1 iron templates and their so kindly suggestions on the spectral fitting. Funding for the creation and distribution of the SDSS Archive has been provided by the Alfred P. Sloan Foundation, the Participating Institutions, the National Aeronautics and Space Administration, the National Science Foundation, the US Department of Energy, the Japanese Monbukagakusho, and the Max Planck Society. The SDSS Web site is <http://www.sdss.org>. The SDSS is managed by the Astrophysical Research Consortium for the Participating Institutions. The Participating Institutions are the University of Chicago, Fermilab, the Institute for Advanced Study, the Japan Participation Group, The Johns Hopkins University, the Korean Scientist Group, Los Alamos National Laboratory, the Max Planck Institute for Astronomy, the Max Planck Institute for Astrophysics, New Mexico State University, the University of Pittsburgh, the University of Portsmouth, Princeton University, the United States Naval Observatory, and the University of Washington. This research has made use of the NED database, which is operated by the Jet Propulsion Laboratory, California Institute of Technology, under contract with the National Aeronautics and Space Administration.

References

- Abazajian K. et al., 2005, *AJ*, 129, 1755
Akritas M. G., Bershadsky M. A., 1996, *ApJ*, 470, 706
Akritas M. G., Siebert J., 1996, *MNRAS*, 278, 919
Begelman M. C., Blandford R. D., Rees M. J., 1984, *Rev. Mod. Phys.*, 56, 255
Bian W., Zhao Y., 2004, *MNRAS*, 347, 607
Bian W., Gu Q., Zhao Y., Chao L., Cui Q., 2006, *MNRAS*, 372, 876
Blundell K. M., Beasley A. J., 1998, *MNRAS*, 299, 165
Bonning E. W., Shields G. A., Salviander S., McLure R. J., 2005, *ApJ*, 626, 89
Boroson T. A., 2003, *ApJ*, 585, 647
Boroson T. A., Green R. F., 1992, *ApJS*, 80, 109
Boyle B. J., Shanks T., Croom S. M., Smith R. J., Miller L., Loaring N., Heymans C., 2000, *MNRAS*, 317, 1014
Cardelli J. A., Clayton G. C., Mathis J. S., 1989, *ApJ*, 345, 245
Collin S. et al., 2006, *A&A*, 456, 75
Dasyra K. M. et al., 2007, *ApJ*, 657, 102
Drory N., Salvato M., Gabasch A., Bender R., Hopp U., Feulner G., Pannella M., 2005, *ApJ*, 619, L131
Ferrarese L., Merritt D., 2000, *ApJ*, 539, L9
Franceschini A., Vercellone S., Fabian A. C., 1998, *MNRAS*, 297, 817
Fender R. P., Gallo E., Jonker P. G., 2003, *MNRAS*, 343, L99
Gallo E., Fender R. P., Pooley G. G., 2003, *MNRAS*, 344, 60
Gebhardt K. et al., 2000, *ApJ*, 539, L13
Grandi S. A., 1982, *ApJ*, 255, 25
Greene J. E., Ho L. C., 2005a, *ApJ*, 627, 721
Greene J. E., Ho L. C., 2005b, *ApJ*, 630, 122
Greene J. E., Ho L. C., Ulvestad J. S., 2006, *ApJ*, 636, 56
Greene J. E., Ho L. C., 2006, *ApJ*, 641, L21
Grupe D., Mathur S., 2004, *ApJ*, 606, L41
Heinz S., 2004, *MNRAS*, 355, 835
Heinz S., Sunyaev R. A., 2003, *MNRAS*, 343, L59
Heckman T. M. et al., 2004, *ApJ*, 613, 109
Ho L. C., 2002, *ApJ*, 564, 120
Ho L. C., Peng C. Y., 2001, *ApJ*, 555, 650
Isobe T. et al., 1990, *ApJ*, 364, 104
Kaspi S., Maoz D., Netzer H., Peterson B. M., Vestergaard M., Jannuzi B.T., 2005, *ApJ*, 629, 61
Kaspi S., Smith P. S., Netzer H., Maoz D., Jannuzi B.T., Giveon U., 2000, *ApJ*, 533, 631
Kauffmann G. et al., 2003, *MNRAS*, 346, 1055
Kellermann K. I., Sramek R., Schmidt M. et al., 1989, *AJ*, 98, 1195
Komossa S., Voges W., Xu D. et al., 2006, *AJ*, 132, 531
Komossa S., Xu D., 2007, 667, L33
Lacy M. et al., 2001, *ApJ*, 551, L17
Laor A., 2000, *ApJ*, 543, L111
Laor A., 2003, astro-ph/0312417
Lauer T. R. et al., 2007, *ApJ*, 622, 808
LaValley M. P., Isobe T., Feigelson E. D., 1992, *BAAS*, 24, 839
Liu Y., Jiang D. R., Gu M. F., 2006, *ApJ*, 637, 669
McLure R. J., Jarvis M. J., 2004, *MNRAS*, 353, L45
Merloni A., Heinz S., Di Matteo T., 2003, *MNRAS*, 345, 1057
Merloni A. et al., 2006, *New Astr.* 11, 567
Nelson C. H., 2001, *ApJ*, 544, L91
Nelson C. H., Whittle M., 1996, *ApJ*, 465, 96
Netzer H. et al., 2006, *A&A*, 453, 525
Netzer H., Trakhtenbrot B., 2007, *ApJ*, 654, 754
O'Donnell James E., 1994, *ApJ*, 422, 158
Onken C. A. et al., 2004, *ApJ*, 615, 645

- Peterson B. M. et al., 2004, ApJ, 613, 682
Panessa F. et al., 2007, A&A, 467, 519
Richards G. T. et al., 2006, ApJS, 166, 470
Sandage A., 1965, ApJ, 141, 1560
Salviander S. et al., 2007, ApJ, 622, 131
Schneider D. P. et al., 2005, AJ, 130, 367
Shen J.-J. et al., 2008, AJ, 135, 928
Shields J. C. et al., 2003, ApJ, 583, 124
Sikora M., Stawarz L., Lasota J., 2007, ApJ, 658, 851
Storey P. J., Hummer D. G., 1995, MNRAS, 272, 41
Strittmatter P. A., Hill P., Pauliny-Toth I. I. K. et al., 1980, A&A, 1980, 88, L12
Sulentic J. W., Marziani P., Dultzin-Hacyan D., 2000, ARA&A, 38, 521
Terashima Y., Wilson A.S., 2003, ApJ, 583, 145
Treu T., Malkan M. A., Blandford R. D., 2004, ApJ, 615, L97
Tremaine S. et al., 2002, Ap J, 574, 740
Vanden B., Daniel E., Shen J. J. et al., 2006, AJ, 131, 84
Whalen D. J., Laurent-Muehleisen S. A., Moran E. C., Becker R. H., 2006, AJ, 131, 1948
Wang J. M., Luo B., Ho L. C., 2004, ApJ, 615, L9
Wang R., Wu X. B., Kong M. Z., 2006, ApJ, 645, 890
Wills B. J., Browne I. W. A., 1986, ApJ, 302, 56
Woo J. H., Urry C. M., 2002, ApJ, 581, L5
Woo J. H. et al., 2006, ApJ, 645, 900
Xu C., Livio M., Baum S. A., 1999, AJ, 118, 1169
Wu X.-B., Wang R., Kong M. Z., Liu F. K., Han J. L., 2004, A&A, 424, 793
Yuan F., Cui W., 2005, ApJ, 629, 408
Zhou H. Y. et al., 2006, ApJS, 166, 128
Zhou H., Wang T., 2002, Chin. J. Astron. Astrophys. (ChJAA), 2, 501